In Situ Single-Cell Bacterial Imaging Provides Mechanistic Insight into the Photodynamic Action of Photosensitizer-loaded Hydrogels

Ingrid V. Ortega, Tuğçe Şener Raman, Agnes Schulze, and Cristina Flors*

In Situ Single-Cell Bacterial Imaging Provides Mechanistic Insight into the Photodynamic Action of Photosensitizer-loaded Hydrogels

*Ingrid V. Ortega,[1] Tuğçe Ş. Raman,[2] Agnes Schulze,[2] Cristina Flors[1,3]**

[1]Madrid Institute for Advanced Studies in Nanoscience (IMDEA Nanociencia), C/ Faraday 9, Madrid 28049, Spain

[2]Leibniz Institute of Surface Engineering (IOM), Permoserstraße 15, 04318 Leipzig, Germany.

[3]Nanobiotechnology Unit Associated to the National Center for Biotechnology (CNB-CSIC-IMDEA), C/ Faraday 9, Madrid 28049, Spain

KEYWORDS: antibacterial hydrogels, photodynamic, single-cell imaging, Min oscillations, PEGDA, wound dressing, transparent hydrogels

ABSTRACT

Hydrogels, three-dimensional hydrophilic polymeric networks with high water retaining capacity, have gained prominence in wound management and drug delivery due to their tunability, softness, permeability and biocompatibility. Electron-beam polymerized polyethylene glycol diacrylate (PEGDA) hydrogels are particularly useful for phototherapies such as antimicrobial photodynamic therapy (aPDT) due to their excellent optical properties. This work takes advantage of the transparency of PEGDA hydrogels to investigate bacterial responses to aPDT at the single-cell level, in real-time and *in situ*. The photosensitizer methylene blue (MB) was loaded in PEGDA hydrogels using two methods: reversible loading and irreversible immobilization within the 3D polymer network. MB release kinetics and singlet oxygen generation were studied, revealing distinct behaviors of both hydrogels. Real-time imaging of *Escherichia coli* was conducted during aPDT in both hydrogel types, using the Min protein system to report changes in bacterial physiology. Min oscillation patterns provided mechanistic insights into bacterial photoinactivation, revealing a dependence on the hydrogel preparation method. This difference was attributed to the mobility of MB within the hydrogel, affecting its direct interaction with bacterial membranes. These findings shed light on the complex interplay between hydrogel properties and bacterial response during aPDT, offering valuable insights for the development of antibacterial wound dressing materials. The study demonstrates the capability of real-time, single-cell fluorescence microscopy to unravel dynamic bacterial behaviors in the intricate environment of hydrogel surfaces during aPDT.

1. Introduction

Hydrogels are three-dimensional hydrophilic polymeric networks with high water retaining capacity. These materials are becoming important as a promising solution for wound management due to their tunability, softness, permeability, biocompatibility or biodegradability.[1-3] In the context of drug delivery, hydrogels benefit from their porosity, which enables drug encapsulation within the 3D polymeric network. Some antibacterial hydrogels have been particularly valuable in the context of light-induced therapies such as antimicrobial photodynamic therapy (aPDT).[4-14] aPDT combines light, molecular oxygen and a photosensitizer to generate reactive oxygen species (ROS) that oxidize lipids, proteins, DNA, and other biomolecules, leading to bacterial inactivation.[15-18] Good transparency is therefore needed for hydrogels to perform well in aPDT, especially for wound dressing applications, and previous work has focused on optimizing their optical properties.[19,20] It was shown that electron-beam polymerized polyethylene glycol diacrylate (PEGDA) hydrogels have a higher transmittance over a broader wavelength range compared to their UV-cured counterparts, reaching values well above 90%.[20]

While aPDT is becoming increasingly popular due to the threat of multidrug resistance, mechanistic questions remain about the inflicted functional changes to bacteria.[15,17] Mechanistic information is particularly difficult to obtain in complex environments such as the hydrogel surface. Taking advantage of the excellent transparency of electron-beam polymerized PEGDA hydrogels developed for aPDT, we have used advanced fluorescence microscopy to gain mechanistic understanding of the interaction between bacteria and photosensitizer-loaded hydrogels *in situ*. We show that the optical properties of these hydrogels are suitable to monitor bacterial death processes at the single-cell level and in real-time. To that end, we have used the

Min protein system, a cell division regulator in *Escherichia coli*, to report changes in bacterial physiology.[21] Under normal growth conditions, MinD is associated with the membrane and undergoes pole-to-pole oscillations.[22] The period of these oscillations is affected by environmental stress factors such as (sublethal) concentrations of antibiotics or mechanical stress,[21,23-25] and likely reflects changes in membrane potential.[21] The use of Min oscillations as a reporter has also been explored in the context of aPDT, showing that the oscillation pattern is sensitive to photosensitizer concentration, and can report on mild photodynamic effects that are overlooked by traditional methods.[26] Herein, we use a similar strategy to compare the real-time response of bacteria to PEGDA hydrogels cross-linked by electron-beam polymerization, in which MB has been incorporated by two different methods: reversible loading and irreversible immobilization within the 3D polymer network.[20] By quantitatively studying Min oscillation patterns of individual bacteria, we gain valuable insights into the underlying mechanism of bacterial photoinactivation, which we find is dependent on the hydrogel preparation method.

2. Experimental Section

2.1 Hydrogel preparation.

Hydrogels were prepared as previously described.[20] Briefly, formulations containing 30 % wt PEGDA (M_w = 700 g/mol, Sigma-Aldrich) in PBS (pH = 7.4) were mildly stirred at 60 ºC to achieve a homogenous solution. After 0.5 h, 400 µL of the formulation was slowly injected with a micropipette into a mold, built from polystyrene petri dishes of 35 x 10 mm with the lid on the top to enable a uniform hydrogel thickness. The formulations were polymerized by an electron beam using a 10 MeV linear electron accelerator (MB10-30 MP, Mevex Corp, Stittville, ON,

Canada). An irradiation dose of 6 kGy was applied for 2.1 s. After cross-linking, hydrogels were taken out from the molds and immersed in PBS. The solution was replaced twice with PBS and twice with Milli-Q water, every hour for a total of 4 h to remove unreacted monomers. Finally, samples were dried for 24 h at 40 ºC. The resulting hydrogels had an average thickness of 185 µm measured by an MCR300 rheometer (Anton Paar, Graz, Austria) with a planar 10 mm diameter probe.

Hydrogels containing MB were produced using two methods (Scheme 1):

- Addition of MB after polymerization (reversible loading)*:* after electron-beam polymerization of the hydrogels, samples of 14 mm diameter were immersed in 5 mL of the photosensitizer MB (Sigma Aldrich) solutions of the desired concentration for 48 h in the dark. Analysis of MB uptake was determined by measuring the maximum absorbance of the solution at 666 nm before, during and after immersion using an Infinite M200 reader (Tecan, Maennedorf, Switzerland).

- Addition of MB before polymerization (irreversible loading): MB was added to the PEGDA formulation before injection into the molds, and the formulation was then polymerized using similar conditions as described above. This preparation method resulted in MB being irreversibly immobilized within pockets of the 3D polymer network.

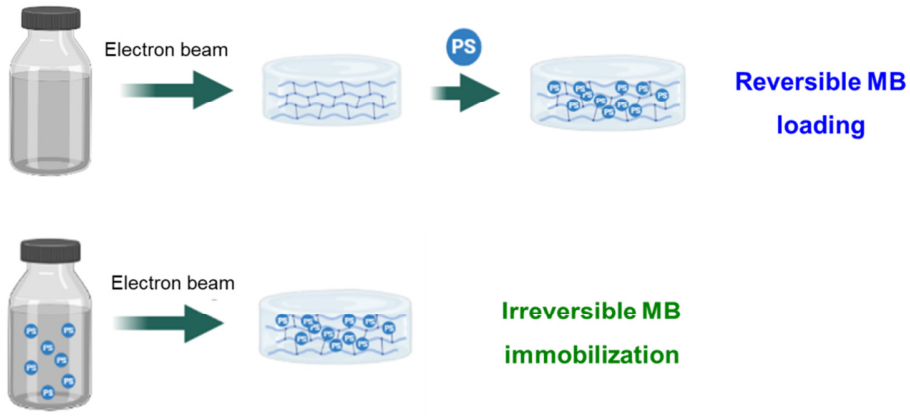

Scheme 1. Two different MB loading methods for electron-beam polymerized PEGDA hydrogels.

2.2 MB release kinetics and singlet oxygen generation

MB loaded hydrogels were immersed in 5 mL PBS solution to release the dye from hydrogels. MB absorbance at 666 nm at different time intervals was measured with an Infinite M200 reader until the solution reached the equilibrium concentration of MB.

The generation of singlet oxygen ($^1O_2$) was determined using the fluorescent probe 9,10-anthracenediyl-bis(methylene) dimalonic acid (ABDA, Sigma-Aldrich), which selectively reacts with $^1O_2$ to form a nonfluorescent product.[4,7] Dried hydrogels (MB-loaded and control) were placed in a well plate containing 5 mL of 0.5 mM ABDA solution. The plate was irradiated with a 660 nm and 940 mW LED (Thorlabs, Newton, USA) placed 10 cm above the sample (1.1 $mW \cdot cm^{-2}$). Aliquots (100 µl) were taken every 5 min within the first hour and then every 30 min for 2 h, and were replaced with PBS. The fluorescence of ABDA at 422 nm was observed with an Infinite M200 reader.

2.4 Bacterial culture

E. coli DH10β were transformed with pDR122 plasmid (GFP-MinD, MinE),[22] grown and recombinant proteins expressed as previously described.[26] 20 μL of bacterial cells were immobilized on a coverslip coated with poly-L-lysine.[26] Hydrogel samples were placed on top of immobilized bacteria and immediately imaged by fluorescence microscopy.

2.5 Fluorescence microscopy and image analysis

Single-cell, real-time fluorescence imaging was performed as previously described.[26] Briefly, images were collected through an inverted optical microscope Nikon Eclipse Ti with a total internal reflection objective (60×, 1.49 NA oil immersion Nikon) and an Electron Multiplying CCD camera (EMCCD) (iXon Ultra897, Andor Technology). Samples were excited by laser irradiation (Omicron Laserage Luxx 488 nm at 20 $W \cdot cm^{-2}$ for GFP). Imaging frames were collected at 3 s intervals and 200 ms integration time. To reduce photobleaching, a shutter (SHB05T-Ø1/2″, Thorlabs) connected to a wave generator (TTi TG330) and synchronized with the EMCCD camera, was used to restrict the irradiation that reached the sample. During some periods of the imaging experiment (see below), a red light emitting diode (LED)(660 nm, ILH-ON04-HYRE-SC201-WIR200, Intelligent LED Solutions) was used to activate MB.

All movies were acquired with Andor Solis. GFP-MinD oscillations along each pole were analyzed by measuring the average fluorescence intensity from a region of 4 × 4 pixels at one pole of the bacterium for all imaging frames. Fluorescence intensity data at each pole were fitted with a damped sine wave to obtain the Min oscillation period for each bacterium, as previously described.[26] Kymographs were generated with Kymograph Builder plugin in Fiji. Statistical analysis of differences between groups was performed using a t-test and considered statistically significant when $p < 0.05$ (*) and $p < 0.01$ (**). Data were analyzed using GraphPad Prism 9.0.

3. Results and Discussion

3.1 Kinetics of MB release and singlet oxygen generation

Loaded hydrogels were initially characterized to determine the relevant timescale for MB release and $^1O_2$ evolution. Figure 1 shows the release profile for both types of hydrogels, which is markedly different. Hydrogels in which MB was added before polymerization liberated only a minimal amount of MB into the solution, maintaining their color even after 24 h of immersion in PBS. On the other hand, reversibly loaded hydrogels released significantly higher amounts of MB, a process that occurred within the first 3 h and reached a plateau after 20 h, with a concomitant loss of color. These results confirm that MB diffusion depends strongly on the method used to incorporate the photosensitizer into the hydrogel matrix, and can be tuned depending on the application.[20] Incorporation of MB before polymerization with an electron-beam produces an encapsulation or even grafting of the dye within the polymer network,[20,27,28] limiting its diffusion, whereas uploading the dye after polymerization results in a much faster release into the medium. [20,27,28]

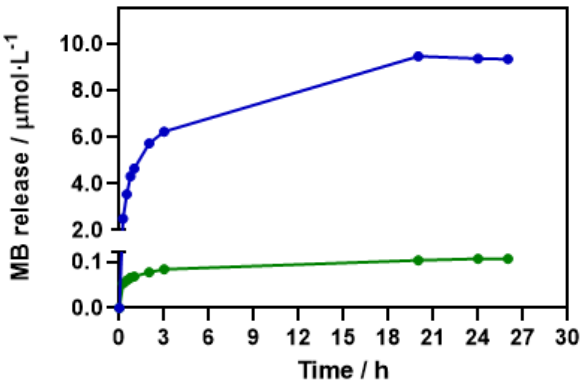

Figure 1. Release of MB from reversibly- (blue) and irreversibly-loaded (green) hydrogels. Hydrogels were loaded at 10 µM MB.

The generation of photosensitized $^1O_2$ from MB in both hydrogels was determined using the fluorescent probe ABDA, which selectively and irreversibly reacts with $^1O_2$ (see Experimental Section). Although $^1O_2$ is typically considered the most relevant ROS in aPDT, it is worth noting that MB has been shown to produce other ROS as well.[29,30] Figure 2 shows that ABDA rapidly reacted with $^1O_2$ within the first 30 min of MB irradiation in both hydrogels, but its consumption was faster in the reversibly-loaded hydrogel, consistent with the MB release profile observed in Figure 1. Indeed, ABDA can react with $^1O_2$ produced by MB released from the hydrogels, but encapsulated MB also photosensitizes $^1O_2$ that can diffuse from the hydrogel into the ABDA solution. As a control, only a slight consumption of ABDA was observed when using a non-loaded hydrogel, presumably due to probe photobleaching (Figure 2). These results confirm that $^1O_2$ is successfully released from hydrogels, and are useful to establish a time window for the real-time fluorescence microscopy experiments below.

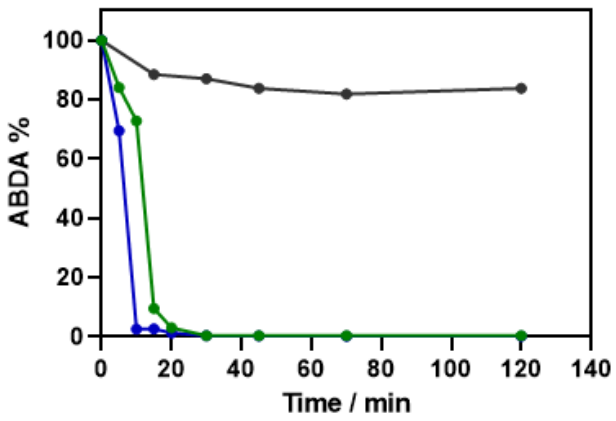

Figure 2. ABDA degradation by $^1O_2$ photosensitized by MB in reversibly- (blue), irreversibly-loaded (green) and control (gray) hydrogels.

3.2 Real-time single bacterial imaging in hydrogels

The changes in the oscillation pattern of the Min system in *E. coli* were used to monitor bacterial stress responses to photodynamic treatment in hydrogels.[21] First, we tested the suitability of both MB-containing hydrogels for *in situ* imaging at the single bacterial level. Figure 3 shows that it is possible to record the oscillation of GFP-MinD in single bacterial cells in both types of hydrogels loaded with MB 0.3 mM. While the acquired movies have somewhat higher background than in previous imaging experiments of immobilized bacteria in solution,[26] the transparency of the PEGDA polymer is high enough for these advanced microscopy experiments, and the presence of MB does not generate significant background at the imaging wavelengths. Indeed, the GFP-MinD fluorescence signal is well above background and can be readily fitted by a damped sinusoidal function (see Experimental Section).

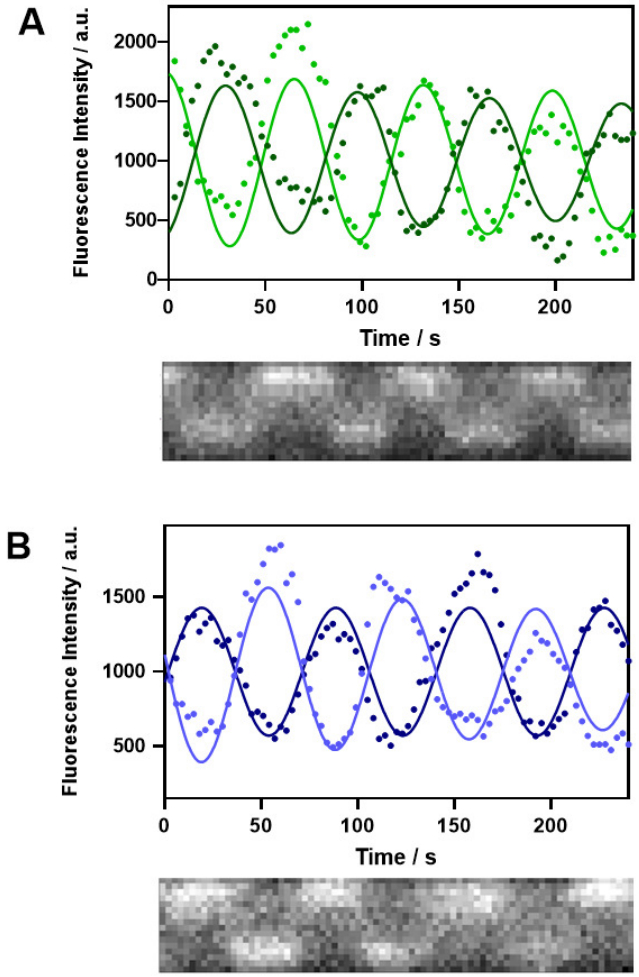

Figure 3. Min oscillations in *E. coli* expressing GFP-MinD in irreversibly- (green, A) and reversibly-loaded (blue, B) MB hydrogels. The top graphs represent the fluorescence intensity vs time along each pole of a single bacterial cell. Below, corresponding kymographs (the entire y-axis corresponds to 1.8 μm).

We next evaluated the evolution of bacterial physiology in the hydrogels upon irradiation of the incorporated MB. Bacteria were first imaged during 4 minutes exciting only with the 488 nm imaging laser (a wavelength that excites GFP and is not significantly absorbed by MB), in order to establish a baseline behavior. Then, a 660 nm LED was turned on to irradiate MB during 20

minutes, since this is the timescale in which most $^1O_2$ is produced (Figure 2). During that irradiation period, 4-minute movies were acquired at the start and before the end of irradiation. After the 660 nm LED was turned off, bacteria were left in the dark for 6 minutes and a final movie was acquired post-irradiation, since we have previously shown that it can take up to 10-20 minutes for the activation of stress responses or metabolic changes that lead to an observable change in the oscillation period.[25]. Figure 4 shows a representative behavior for a bacterium in an irreversibly-loaded hydrogel during the imaging steps described above. It can be clearly seen that the oscillation period increases immediately after MB irradiation, and becomes even slower as the experiment progresses. Violin plots incorporating data from tens of bacteria (Figure 5) show a significant increase in the Min oscillation period by about 10 s immediately after the start of red LED irradiation (from 60.6 s to 71.0 s). After 20 minutes of irradiation, the oscillation time markedly increased by an average of 22 s more. Incubation of a few minutes without irradiation led to an even more pronounced effect on Min oscillations, with an average oscillation time of 122.8 s, accompanied by a significant increase in cell-to-cell variability.

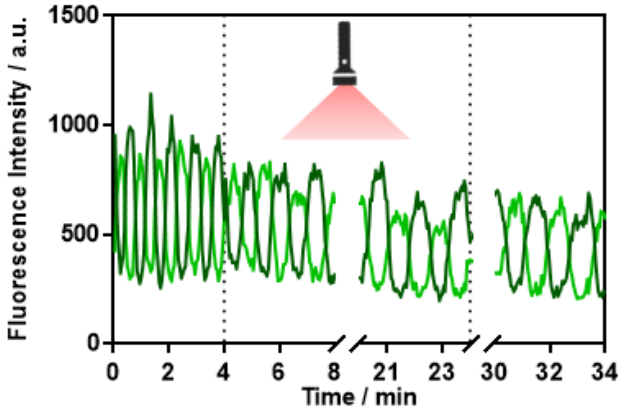

Figure 4. Min oscillatory behavior for a bacterium in an irreversibly-loaded hydrogel during the imaging steps described in the text, showing the period of red light LED irradiation.

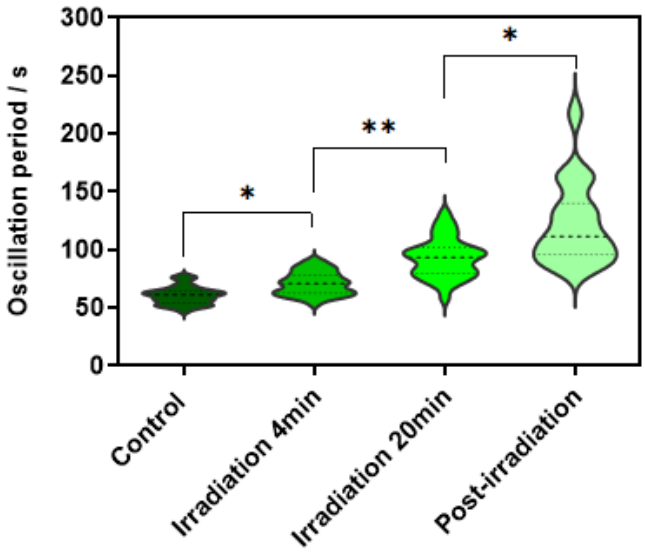

Figure 5. Effect of MB in irreversibly-loaded hydrogels on Min oscillation period at different points of the imaging sequence (n = 34). Significant differences (*) ($p < 0.05$) and (**) ($p < 0.01$).

When a similar experiment was performed in reversibly-loaded hydrogels, the evolution of Min oscillation was remarkably different, and bacterial behavior could be classified in two groups (Figure 6). In the first group (A), which represented 36% of the population, the oscillation period increased slightly upon the start of red LED irradiation, and then it kept stable until the end of the experiment. This could be observed more clearly in the corresponding violin plots (Figure 7), and suggests only a small impact of the photodynamic treatment on bacterial physiology (at least in the observed timescale). In the other group (B), representing the majority of the bacterial cells studied (64%), the oscillation abruptly stopped before the end of the experiment (Figure 6B). As a control, it was confirmed that for bacterial cells exposed to non-loaded hydrogels under the

same experimental conditions, the Min oscillation pattern remained stable during the experiment, and thus bacterial physiology was not affected (Figure 8).

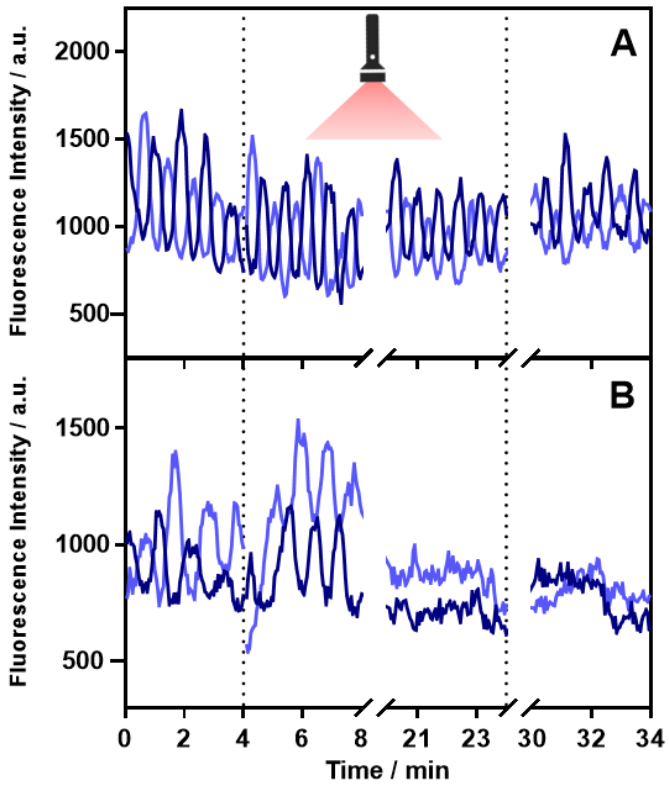

Figure 6. Min oscillatory behavior for individual bacteria in a reversibly-loaded hydrogel during the imaging steps described in the text, showing the period of red light LED irradiation. The oscillatory patterns shown represent about 36% (A) and 64% (B) of the population. In B, the fluorescence intensity at each pole is slightly different.

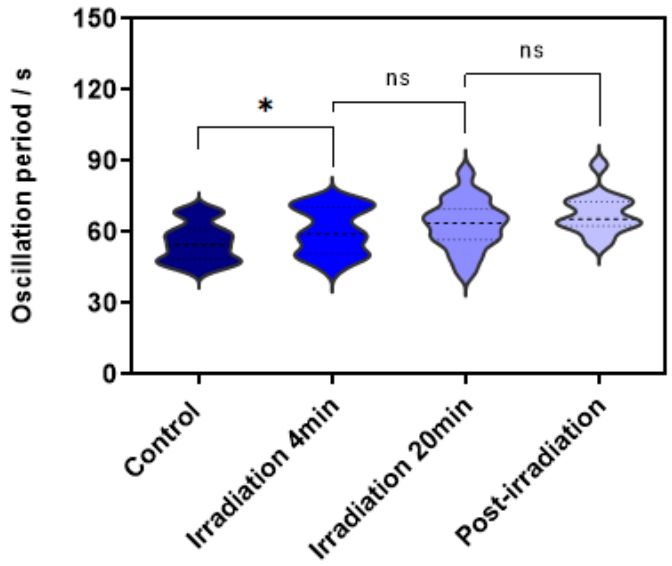

Figure 7. Effect of MB in reversibly-loaded hydrogels on Min oscillation period at different points of the imaging sequence (n = 39 for the first control group, however as seen in Figure 6B not all bacteria remain oscillating until the end of the imaging sequence). Significant differences (*) ($p < 0.05$).

The above results show that *in situ* imaging in hydrogels in real-time and at the single bacterial level can reveal differences in bacterial behavior depending on the characteristics of the hydrogel. In hydrogels loaded with MB irreversibly, the Min oscillation periods significantly increases upon irradiation, while for those loaded reversibly the oscillation period increases only slightly or ceases abruptly. It is interesting to compare this behavior with our previous study on the effect of aPDT treatment on Min oscillations, which was carried out on bacteria immersed in a MB solution.[26] In that work, the Min oscillation pattern closely resembled that of hydrogels loaded reversibly (Figure 6B), i.e. the oscillation halted abruptly (instead of slowing down). We hypothesize that for both aPDT in solution[26] and for the majority of bacteria in reversibly-loaded hydrogels, MB has direct contact with the bacterial membrane, leading to a more pronounced

photodamage that results in an abrupt interruption of the oscillation. On the other hand, when MB is irreversibly immobilized in the polymer pockets, $^1O_2$ (or other ROS) diffuse from the hydrogel to the bacteria on the surface. The diffusion length of $^1O_2$ is likely to be similar to that in aqueous solution or a mammalian cell, i.e. 100-150 nm.[31] In this scenario, there is less contact between MB and the bacterial membrane, resulting in a more gradual effect on bacterial physiology that we observe as a slowdown in Min oscillations. The latter situation would also affect some of the bacteria in reversibly-loaded hydrogels (~36%) that have a reduced contact with MB, for which a slight slowdown in the oscillation period is observed. This interpretation is supported by a previous observation that cumulative light excitation slowed down the oscillation by about 10 s,[23] presumably due to light-induced ROS generation by GFP[32] or buffer components.[33] Therefore, changes in the Min oscillation pattern can inform about the different mechanisms of action of aPDT.

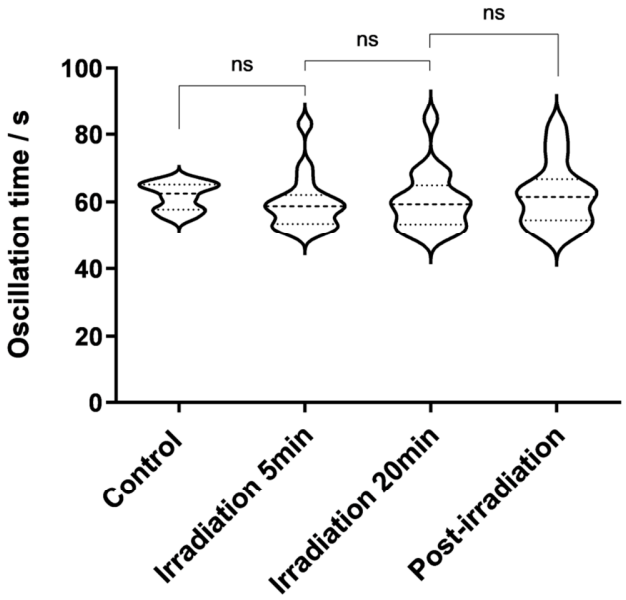

Figure 8. Nonloaded hydrogels produce no significant change in Min oscillation period during the imaging sequence (n = 17).

4. Conclusions

Real-time single-cell fluorescence microscopy methods enable the visualization of stress responses in bacteria with spatiotemporal resolution, reveal hidden dynamics and population heterogeneity, and connect molecular scale mechanisms to cell fate.[34-36] By performing *in situ* advanced fluorescence microscopy on hydrogels with excellent optical properties designed for aPDT applications, we show that it is possible to link mechanistic information about photodynamic action with the hydrogel preparation method. The changes in bacterial physiology during photodynamic treatment depend on the mobility of MB within the hydrogel. In hydrogels with reversible loading, free MB diffusion results in a direct interaction with the bacterial membrane that leads to fast bacterial inactivation. On the other hand, encapsulation of MB within the polymeric network of cross-linked hydrogels mostly precludes a direct interaction between photosensitizer and bacteria. In this case, the primary mechanism likely involves the interaction between photosensitized ROS that diffuse towards the hydrogel surface and affects the bacterial membrane. This information contributes to a better understanding of aPDT mechanisms in the complex environment provided by the hydrogel surface, and may provide design guidelines for the next generation of antibacterial wound dressing materials.

AUTHOR INFORMATION

Corresponding Author

*To whom correspondence should be addressed at cristina.flors@imdea.org.

ACKNOWLEDGMENT

This work was supported by Spanish *Ministerio de Ciencia e Innovación* (PID2021-122231NB-I00, PRE2018-084983, and CEX2020-001039-S). Financial support by the Federal State of Germany, the Free State of Saxony, and the Republic of Turkey Ministry of National Education is gratefully acknowledged. The authors thank Prof. Piet A. J. de Boer (Case Western Reserve University) for the gift of plasmid pDR122.

REFERENCES

(1) Jia, B.; Li, G.; Cao, E.; Luo, J.; Zhao, X.; Huang, H. Recent progress of antibacterial hydrogels in wound dressings. *Mater Today Bio* **2023**, *19*, 100582.

(2) Dsouza, A.; Constantinidou, C.; Arvanitis, T. N.; Haddleton, D. M.; Charmet, J.; Hand, R. A. Multifunctional Composite Hydrogels for Bacterial Capture, Growth/Elimination, and Sensing Applications. *ACS Appl Mater Interfaces* **2022**, *14*, 47323-47344.

(3) Liu, Y.; Ma, Q.; Liu, S.; Lin, D.; Zhao, H.; Liu, X.; Zhou, G. Research progress on antimicrobial hydrogel dressing for wound repair. *Eur. Polym. J.* **2023**, *197*, 112372.

(4) Spagnul, C.; Greenman, J.; Wainwright, M.; Kamil, Z.; Boyle, R. W. Synthesis, characterization and biological evaluation of a new photoactive hydrogel against Gram-positive and Gram-negative bacteria. *J Mater Chem B* **2016**, *4*, 1499-1509.

(5) Elkihel, A.; Vernisse, C.; Ouk, T. S.; Lucas-Roper, R.; Chaleix, V.; Sol, V. Xylan-Porphyrin Hydrogels as Light-Triggered Gram-Positive Antibacterial Agents. *Gels* **2023**, *9*, 124.

(6) Willis, J. A.; Trevino, A.; Nguyen, C.; Benjamin, C. C.; Yakovlev, V. V. Photodynamic Therapy Minimally Affects HEMA-DMAEMA Hydrogel Viscoelasticity. *Macromol Biosci* **2023**, *23*, e2300124.

(7) Glass, S.; Rudiger, T.; Griebel, J.; Abel, B.; Schulze, A. Uptake and release of photosensitizers in a hydrogel for applications in photodynamic therapy: the impact of structural parameters on intrapolymer transport dynamics. *RSC Adv* **2018**, *8*, 41624-41632.

(8) Xu, Y.; Chen, H.; Fang, Y.; Wu, J. Hydrogel Combined with Phototherapy in Wound Healing. *Adv Healthc Mater* **2022**, *11*, e2200494.

(9) Wang, Z.; Fu, L.; Liu, D.; Tang, D.; Liu, K.; Rao, L.; Yang, J.; Liu, Y.; Li, Y.; Chen, H.; Yang, X. Controllable Preparation and Research Progress of Photosensitive Antibacterial Complex Hydrogels. *Gels* **2023**, *9*, 571.

(10) Glass, S.; Kuhnert, M.; Lippmann, N.; Zimmer, J.; Werdehausen, R.; Abel, B.; Eulenburg, V.; Schulze, A. Photosensitizer-loaded hydrogels for photodynamic inactivation of multirestistant bacteria in wounds. *RSC Adv* **2021**, *11*, 7600-7609.

(11) Elkihel, A.; Christie, C.; Vernisse, C.; Ouk, T. S.; Lucas, R.; Chaleix, V.; Sol, V. Xylan-Based Cross-Linked Hydrogel for Photodynamic Antimicrobial Chemotherapy. *ACS Appl Bio Mater* **2021**, *4*, 7204-7212.

(12) Zhang, C.; Yang, D.; Wang, T. B.; Nie, X.; Chen, G.; Wang, L. H.; You, Y. Z.; Wang, Q. Biodegradable hydrogels with photodynamic antibacterial activity promote wound healing and mitigate scar formation. *Biomater Sci* **2022**, *11*, 288-297.

(13) Khurana, B.; Gierlich, P.; Meindl, A.; Gomes-da-Silva, L. C.; Senge, M. O. Hydrogels: soft matters in photomedicine. *Photochem Photobiol Sci* **2019**, *18*, 2613-2656.

(14) Lopez-Lopez, N.; Munoz Resta, I.; de Llanos, R.; Miravet, J. F.; Mikhaylov, M.; Sokolov, M. N.; Ballesta, S.; Garcia-Luque, I.; Galindo, F. Photodynamic Inactivation of Staphylococcus aureus Biofilms Using a Hexanuclear Molybdenum Complex Embedded in Transparent polyHEMA Hydrogels. *ACS Biomater Sci Eng* **2020**, *6*, 6995-7003.

(15) Cieplik, F.; Deng, D.; Crielaard, W.; Buchalla, W.; Hellwig, E.; Al-Ahmad, A.; Maisch, T. Antimicrobial photodynamic therapy - what we know and what we don't. *Crit Rev Microbiol* **2018**, *44*, 571-589.

(16) Wainwright, M.; Maisch, T.; Nonell, S.; Plaetzer, K.; Almeida, A.; Tegos, G. P.; Hamblin, M. R. Photoantimicrobials-are we afraid of the light? *Lancet Infect Dis* **2017**, *17*, e49-e55.

(17) Alves, E.; Faustino, M. A.; Neves, M. G.; Cunha, A.; Tome, J.; Almeida, A. An insight on bacterial cellular targets of photodynamic inactivation. *Future Med Chem* **2014**, *6*, 141-164.

(18) Yan, E.; Kwek, G.; Qing, N. S.; Lingesh, S.; Xing, B. Antimicrobial Photodynamic Therapy for the Remote Eradication of Bacteria. *Chempluschem* **2023**, *88*, e202300009.

(19) Pelras, T.; Glass, S.; Scherzer, T.; Elsner, C.; Schulze, A.; Abel, B. Transparent Low Molecular Weight Poly(Ethylene Glycol) Diacrylate-Based Hydrogels as Film Media for Photoswitchable Drugs. *Polymers (Basel)* **2017**, *9*, 639.

(20) Glass, S.; Kuhnert, M.; Abel, B.; Schulze, A. Controlled Electron-Beam Synthesis of Transparent Hydrogels for Drug Delivery Applications. *Polymers (Basel)* **2019**, *11*, 501.

(21) Ortega, I. V.; Viela, F.; Flors, C. Min oscillations in bacteria as real-time reporter of environmental challenges at the single-cell level. *Open Biol* **2023**, *13*, 230020.

(22) Raskin, D. M.; de Boer, P. A. Rapid pole-to-pole oscillation of a protein required for directing division to the middle of Escherichia coli. *Proc Natl Acad Sci U S A* **1999**, *96*, 4971-4976.

(23) Downing, B. P.; Rutenberg, A. D.; Touhami, A.; Jericho, M. Subcellular Min oscillations as a single-cell reporter of the action of polycations, protamine, and gentamicin on Escherichia coli. *PLoS One* **2009**, *4*, e7285.

(24) del Valle, A.; Torra, J.; Bondia, P.; Tone, C. M.; Pedraz, P.; Vadillo-Rodriguez, V.; Flors, C. Mechanically Induced Bacterial Death Imaged in Real Time: A Simultaneous Nanoindentation and Fluorescence Microscopy Study. *ACS Appl Mater Interfaces* **2020**, *12*, 31235-31241.

(25) Viela, F.; Ortega, I. V.; Hernandez, J. J.; Rodriguez, I.; Moreno-Da Silva, S.; López-Moreno, A.; Pérez, E. M.; Flors, C. Real-Time Imaging of the Mechanobactericidal Action of Colloidal Nanomaterials and Nanostructured Topographies. *Small Sci.* **2023**, *3*, 2300002.

(26) Ortega, I. V.; Torra, J.; Flors, C. Min Oscillations as Real-time Reporter of Sublethal Effects in Photodynamic Treatment of Bacteria. *ACS Infect Dis* **2022**, *8*, 86-90.

(27) Schmidt, M.; Abdul Latif, A.; Prager, A.; Glaser, R.; Schulze, A. Highly Efficient One-Step Protein Immobilization on Polymer Membranes Supported by Response Surface Methodology. *Front Chem* **2021**, *9*, 804698.

(28) Schmidt, M.; Zahn, S.; Gehlhaar, F.; Prager, A.; Griebel, J.; Kahnt, A.; Knolle, W.; Konieczny, R.; Glaser, R.; Schulze, A. Radiation-Induced Graft Immobilization (RIGI): Covalent Binding of Non-Vinyl Compounds on Polymer Membranes. *Polymers (Basel)* **2021**, *13*, 1849.

(29) Garcia-Diaz, M.; Huang, Y. Y.; Hamblin, M. R. Use of fluorescent probes for ROS to tease apart Type I and Type II photochemical pathways in photodynamic therapy. *Methods* **2016**, *109*, 158-166.

(30) Tardivo, J. P.; Del Giglio, A.; de Oliveira, C. S.; Gabrielli, D. S.; Junqueira, H. C.; Tada, D. B.; Severino, D.; de Fatima Turchiello, R.; Baptista, M. S. Methylene blue in photodynamic therapy: From basic mechanisms to clinical applications. *Photodiagnosis Photodyn Ther* **2005**, *2*, 175-191.

(31) *Singlet Oxygen: Applications in Biosciences and Nanosciences*; Nonell, S., Flors, C., Eds.; Royal Society of Chemistry, 2016; Vol. 1.

(32) Jimenez-Banzo, A.; Nonell, S.; Hofkens, J.; Flors, C. Singlet oxygen photosensitization by EGFP and its chromophore HBDI. *Biophys. J.* **2008**, *94*, 168-172.

(33) Lepe-Zuniga, J. L.; Zigler, J. S., Jr.; Gery, I. Toxicity of light-exposed Hepes media. *J Immunol Methods* **1987**, *103*, 145.

(34) Lagage, V.; Uphoff, S. Pulses and delays, anticipation and memory: seeing bacterial stress responses from a single-cell perspective. *FEMS Microbiol Rev* **2020**, *44*, 565-571.

(35) Choi, H.; Rangarajan, N.; Weisshaar, J. C. Lights, Camera, Action! Antimicrobial Peptide Mechanisms Imaged in Space and Time. *Trends Microbiol* **2016**, *24*, 111-122.

(36) Gollmer, A.; Maisch, T.; Felgentraeger, A.; Flors, C. Real-time imaging of photodynamic action in bacteria. *J. Biophoton.* **2017**, *10*, 264-270.

TOC GRAPH